Arch. Metall. Mater. **70** (2025), 1, 259-268

DOI: https://doi.org/10.24425/amm.2025.152541

Z.-S. NONG[1#], D.-Y. ZHANG[2#*], Y. YU[1]

EFFECT OF LASER QUENCHING ON SURFACE MICROSTRUCTURES OF TA15 TITANIUM ALLOY

In order to improve the mechanical properties of the surface for TA15 titanium alloy, the microstructures evolution of alloys under different laser power were studied by analyzing the transformation of microstructures and the distribution of composition and hardness. The results show that the laser quenching can induce the martensite transformation of TA15 alloy, resulting in the formation of α-Ti and α'-Ti hardening phases on the surface. The morphologies of TA15 are composed of quenched layer, transition region and matrix after laser quenching. The formation of martensite α'-Ti results in the hardening layer and a hardness higher than 430 $HV_{0.3}$ on the surface of TA15 alloy. The thickness and width of the hardening layer increase with the increase of laser quenching power. When the power is 800 W, there will be the maximum thickness and width of 777 μm and 2117 μm, respectively.

Keywords: Laser quenching; Microstructures; Hardening layer

1. Introduction

Titanium alloys are commonly used in aviation industry because of its high hardness, wear resistance, sufficient toughness and dimensional stability and other excellent properties [1-3]. There are three common types of titanium alloys including α, β and α + β type alloy. Ti-6.5Al-2Zr-1Mo-1V alloy (defined as TA15 alloy) is a nearly α type titanium alloy with high aluminum content. The main strengthening mechanism is solution strengthening of α-stable element Al, and β-stable elements Mo and V are added to improve its processability [4-6]. TA15 alloy is usually used for manufacturing long-service aviation parts with operating temperature below 500°C due to its excellent strength at room temperature and high temperature, thermal stability and welding performance [7-9]. However, due to the relatively low hardness of TA15 alloy, its wear resistance cannot meet the requirements of industrial production and application, which limits its further development. Therefore, strengthening the surface of alloy to improve hardness and wear resistance is the focus of research on TA15 alloy.

Heat and surface treatment can improve the hardness and wear resistance of titanium alloy, but the overall mechanical properties of the alloy after heat treatment are also changed [10-13]. Therefore, there are many surface treatment processes developed for titanium alloys. In recent years, the laser quenching treatment, which use the high-energy density laser beam to irradiate the surface of materials, can make the temperature of the laser zone rise sharply, and then with the help of the heat conductivity of the material to cool, so as to achieve quenching on the surface of the material to form a high hardening layer [14-16]. After laser treatment, the deformation is small, and the surface treatment of complex component is easy to carry out. The results of laser quenching for the surface of β-Ti-35Nb-2Ta-3Zr alloy by Zhang et al. [17] show that there are obvious grains coarsening and martensitic transformation after laser quenching. It has a positive effect on the superelasticity of this alloy. In addition, the acicular α' martensite is found in the matrix of α-phase for the pure titanium due to the rapid cooling rate during the process of laser quenching [18]. The investigations of laser quenching on the titanium alloy showed that when the acicular martensite α' phase is formed, and the hardness and wear resistance of the alloy surface were significantly improved, as well as the oxidation resistance [19,20].

In this work, in order to explore the laser quenching process on the surface of TA15 titanium alloy, the surface microstructures of TA15 alloy after different laser quenching treatments were

[1] SHENYANG AEROSPACE UNIVERSITY, SCHOOL OF MATERIALS SCIENCE AND ENGINEERING, SHENYANG 110136, CHINA
[2] SHENYANG AEROSPACE UNIVERSITY, KEY LABORATORY OF FUNDAMENTAL SCIENCE FOR NATIONAL DEFENSE OF AERONAUTICAL DIGITAL MANUFACTURING PROCESS, SHENYANG 110136, CHINA

* Corresponding author: wjdchuifu@163.com
\# These authors contributed equally to this work and should be considered co-first authors

studied, and the influence of laser power on the phase formation, microstructures evolution, composition and hardness distribution of the TA15 alloy was analyzed. This work reveals the hardening effect of quenched layer on the surface of titanium alloy, and provides a simple way for the strengthening of the surface for titanium alloy. The results of this work will be of great significance to guide the surface treatment of titanium alloy and improve the mechanical properties of titanium alloy.

2. Experimental methods

TA15 titanium alloy plate with thickness of 3 mm was selected for laser quenching experiment in this work. The test results of the main chemical components for TA15 alloy by the method of X-ray fluorescence spectrum are shown in TABLE 1, and Fig. 1 shows the corresponding initial microstructures of TA15 alloy. It can be seen that the matrix of TA15 alloy was a typical equiaxed structure, consisting of about 60% primary equiaxed α phases and 40% transformed β structures by calculating the contrast of light and dark in metallographic photographs. The dark colored regions correspond to the typical transformed β structures, usually consisting of some secondary lamellar α phase and a small amount of β phase in TA15 alloy.

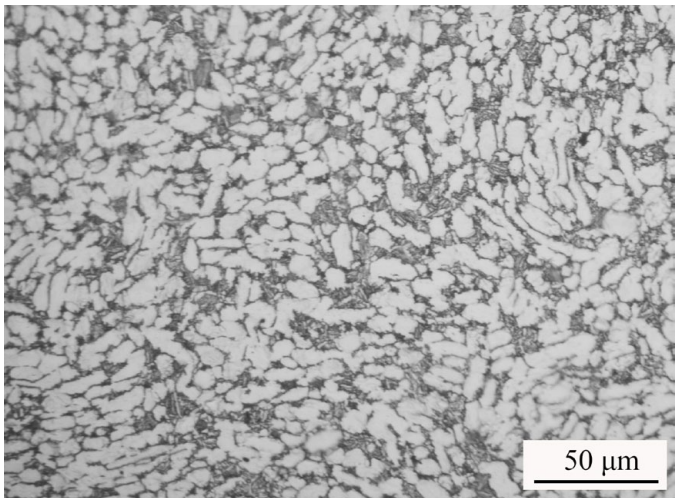

Fig. 1. Microstructures of TA15 initial sample

A cold metal transition welder (TPS 4000CMT) equipped with six-axis robot arm (KR30HA) was used for laser quenching experiment. The fiber laser (RFL-C4000X) with a wavelength of 1080 nm was used as a heat source. During the experiment, the surface of sample was kept in the focal plane and perpendicular to the incident laser beam, and the laser covering head was driven by a mechanical arm for translation. High energy laser beam was used in this experiment, and the spot diameter is set to 2 mm. The scanning speed used for laser quenching was 1.0 m/min, and the power was set to 500 W, 600 W, 700 W, and 800 W. All laser quenching processes of this work were carried out under the protection of argon with a gas flow rate of 20 L/min. Before laser quenching, the surface of the TA15 sample was polished. Fig. 2 shows the schematic diagram of laser quenching experiment in this work. The samples, which were selected in the center of the laser quenching path, were prepared by wire cutting along the direction perpendicular to the laser treatment. Prior to microstructures observation and phase composition analysis, the surface and cross-section of the samples were sanded and polished, and then etched with the reagent with a volume percentage ratio of $HF:HNO_3:H_2O = 2:3:95$. The X-ray diffractometer (D8 ADVANCE) was adopted to analyze phase compositions of alloys, in which Cu with the wavelength of 1.541 nm is used as the target material for X-ray sources. The tested voltage and current are 45 kV and 200 mA respectively. The scanning range was 20°~80° with the scanning speed of 5°/min. The OLYMPUS GX71 optical microscope (OM) and ZEISS-14-type scanning electron microscope (SEM) with the energy dispersive spectrometer (EDS) were introduced to observe the microstructures and analyze the element distribution of the alloy. In the SEM characterization, a secondary electron probe was used with an accelerating voltage of 15 kV. The working distance of the electron microscope was 7.9 mm. The micro Vickers hardness tester (MHV-1000Z) was used to measure the hardness of the processed surface of TA15 alloy. After preliminary test result, the test load in this work was set as 300 g and the loading time was set to 15 s. Before hardness testing, the metallographic preparation which has been described above for the processed surface of samples was also carried out to maintain the surface flatness. The spacing between the indentations is about 0.5 mm in this work.

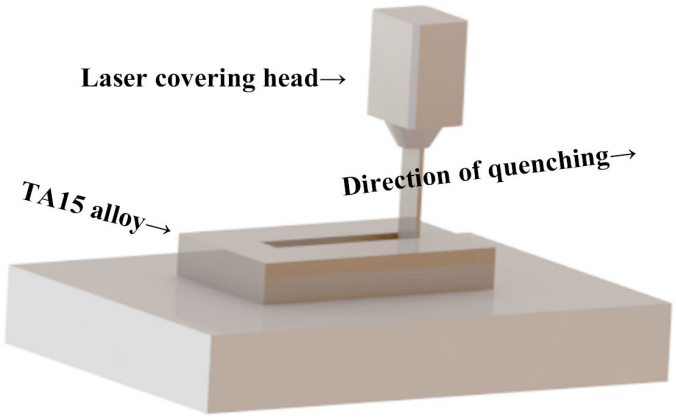

Fig. 2. Schematic diagram of laser surface quenching

TABLE 1

Chemical composition of TA15 titanium alloy (wt.%)

Ti	Al	V	Mo	Zr	C	Fe	Si	O	N	H
Other	6.83	2.26	1.81	2.22	0.006	0.047	0.024	0.11	0.006	0.0025

3. Results and discussions

3.1. Effect of laser quenching on phase structures

Fig. 3 is the XRD pattern of TA15 alloy at initial state and after different laser power treatment. Comparing with the initial state, the diffraction peaks of TA15 alloy after different treatments are basically the same, which are all composed of α (PDF#44-1294) and α' (PDF#51-0631) with hexagonal closely packed (HCP) structure. Because the indicated maximum for the β phase with body-centered cubic (BCC) structure around the angles of 38 degrees is in the position of the maximum indicated for the α phase, and there are no other diffraction peaks related to the β phase being calibrated, hence, the β phase in this TA15 alloy cannot been identified. This may be attributed to the low content of β phase in the alloy after laser quenching treatment. The locations of the diffraction peak for α phase are consistent with that of TA15 alloy powder [21] and alloy after thermomechanical processing [22]. It indicates that the matrix structure of TA15 alloy after surface laser quenching remains unchanged. Due to the rapid cooling rate of laser quenching, there is a large temperature gradient in the quenching zone. The Ms (martensitic start) temperature of metastable β titanium is easily reached during the quenching process, resulting in induced martensitic transformation. Hence, the α'-Ti can be formed through nondiffused shear in the process of cooling. This is the same as the mechanism of martensitic transformation of pure titanium after laser quenching [18]. The absence of α'-Ti diffraction peaks in the initial state also confirms it. The full width at half maximum (FWHM) of the diffraction peaks for α' phase were measured, and the FWHM of α' phase after 500 W, 600 W, 700 W, and 800 W laser quenching are 0.236°, 0.266°, 0.283° and 0.289°, respectively. It can be seen that with the increase of laser quenching power, the FWHM of α' phase gradually increases, which indicates that the larger the laser quenching power, the greater the lattice distortion of the

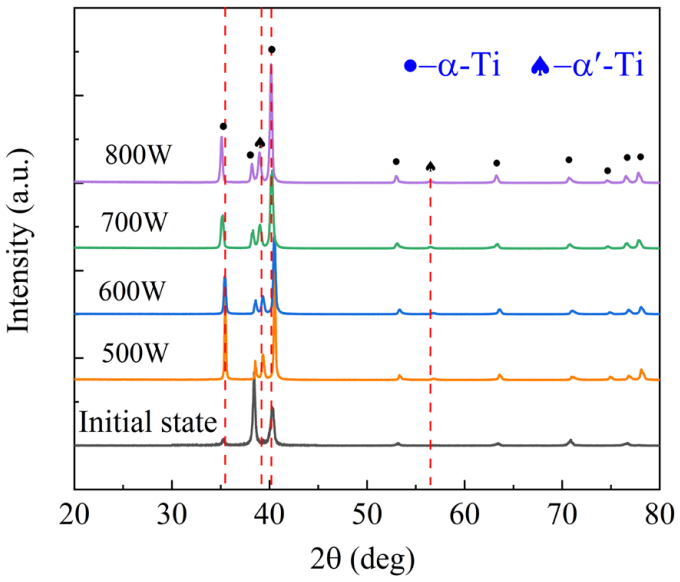

Fig. 3. XRD pattern of TA15 alloy at initial state and after different laser quenching treatment

martensite in TA15 alloy. The calculated lattice constants of α-Ti based on the XRD diffraction peaks are shown in TABLE 2. The lattice constants of α'-Ti cannot be evaluated effectively due to the small content. It can be seen from TABLE 2 that the lattice constant of α-Ti increases obviously with the increase of laser power. Moreover, the diffraction peaks of α-Ti and α'-Ti all shift to the left with the increase of laser quenching power, and the corresponding diffraction angles decrease. This is because in the process of laser quenching, the crystal structures of α-Ti and α'-Ti would appear lattice distortion under the irradiation of high-energy laser, which makes the lattice constant large. The residual tensile stress on the surface of the alloy makes the lattice anisotropy shrinks, resulting in the left shift of the diffraction peaks.

TABLE 2

Lattice constants of α-Ti in initial TA15 alloy and alloys after laser quenching

Sample status		a = b (Å)	c (Å)
Initial alloy		2.924	4.670
Alloys after laser surface quenching	500 W	2.927	4.671
	600 W	2.929	4.675
	700 W	2.949	4.690
	800 W	2.952	4.696

3.2. Effect of laser quenching on surface microstructures

Fig. 4a shows the surface morphologies of TA15 alloy after different laser quenching treatment. The typical laser quenching morphologies are observed with uniform quenching layer and no obvious defects. The laser-treated surfaces of alloys exhibit some instability due to the effects of heating and cooling cycles, and different regions with colors including silver grey, grey, brown, and blue are found. There are visible differences in width of laser treated area. The relatively stable morphologies of the middle section of laser treatment indicate the rationality of this laser quenching process in this study. It is found in Fig. 4b and Fig. 4c that the surface and cross section microstructures of the alloy are formed into three regions with different microstructure due to heat transfer, namely, the matrix of the inner layer, the transition region in the middle and the quenched layer of the outer layer. With the increase of quenching depth, the microstructures have a trend of coarsening, which shows that the laser quenching process has a good range of action, about 300-400 μm [20].

Figs. 5-8 show the microstructures of TA15 alloy after the laser power treatment of 500 W, 600 W, 700 W, and 800 W, respectively. It can be found from the microstructures of quenched layer (Fig. 5b-8b) that the main structures are typical hexagonal martensite α'. These microstructures of martensite α' are the same as that observed by Zong et al. [18]. The α' phase is lamellar and the power increase has no significant effect on the morphology of α' phase. The appearance of martensite α' in titanium alloy is due to the fact that the stable element V of high temperature β phase has no time to spread during the rapid cooling of titanium

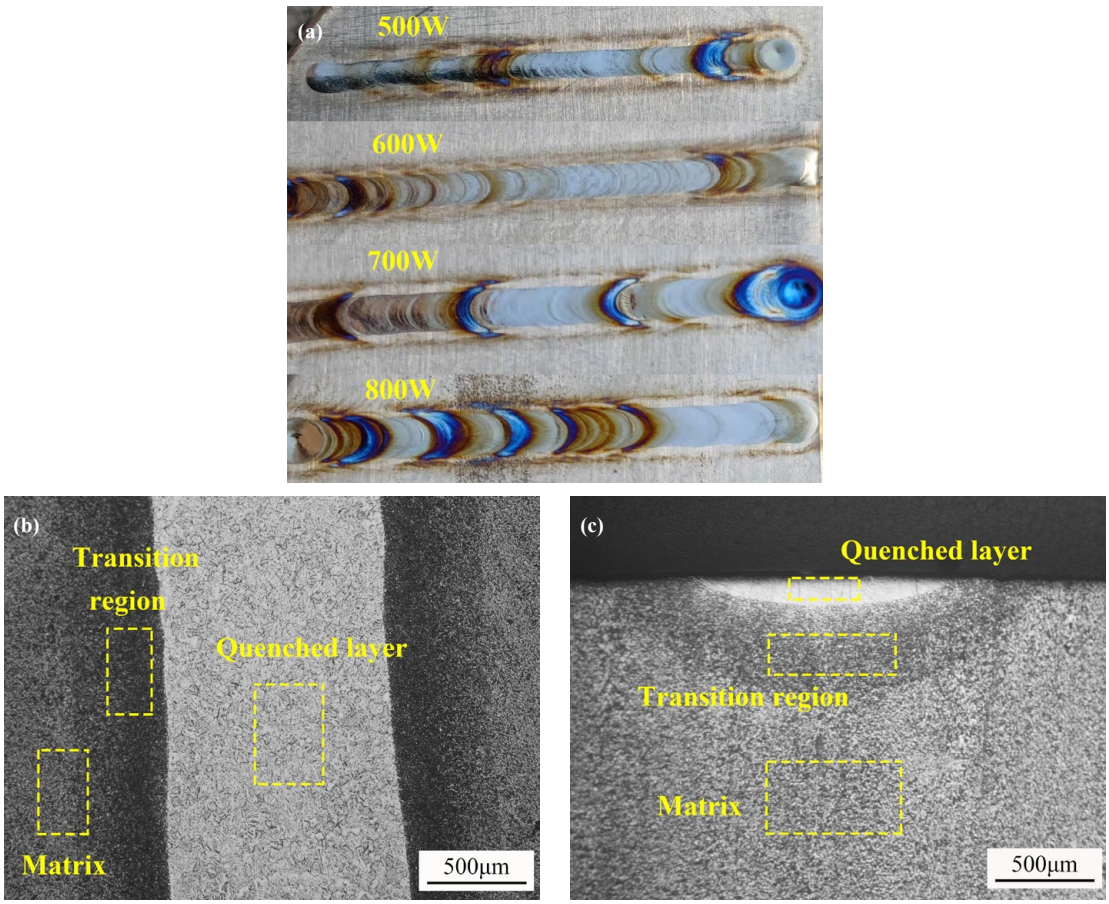

Fig. 4. Macroscopic morphologies (a), surface microstructures (b), and cross section microstructures (c) of TA15 alloy after laser treatment

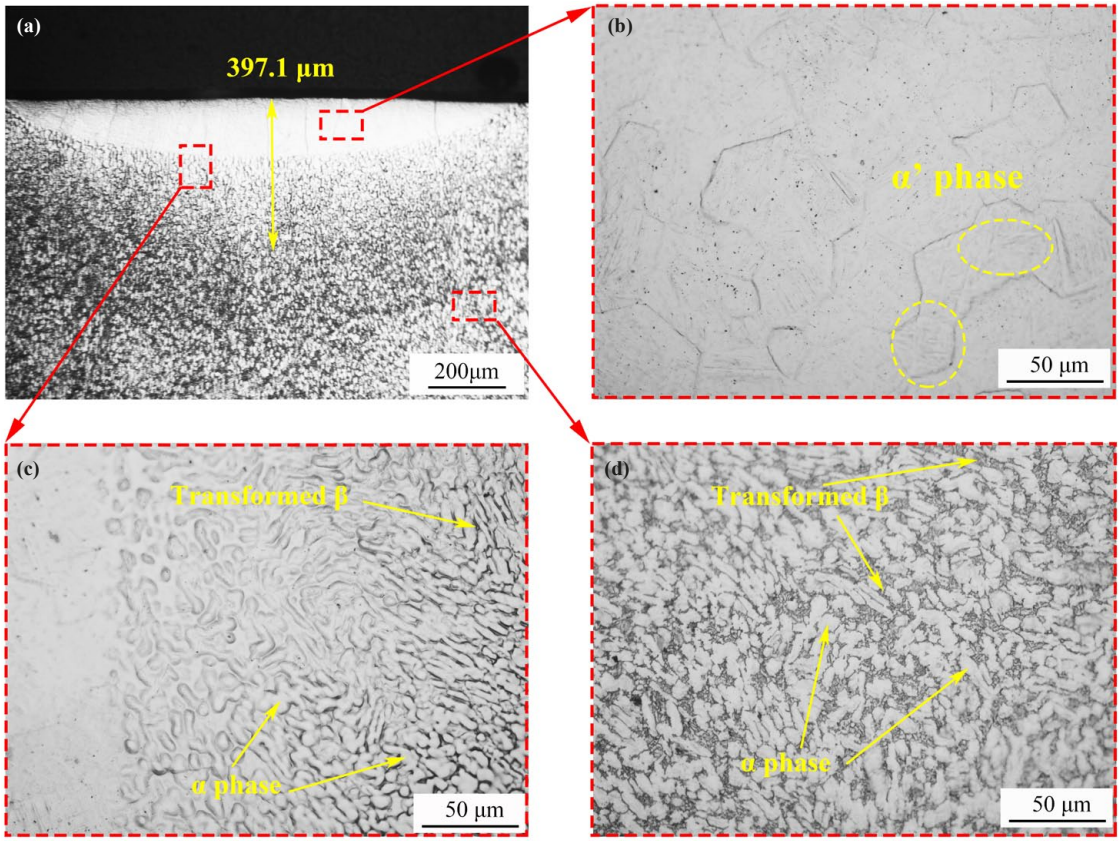

Fig. 5. Cross-section microstructures of the quenched layer (a), microstructures of quenched layer (b), transition region (c), and matrix (d) for TA15 alloy after the laser power treatments of 500 W

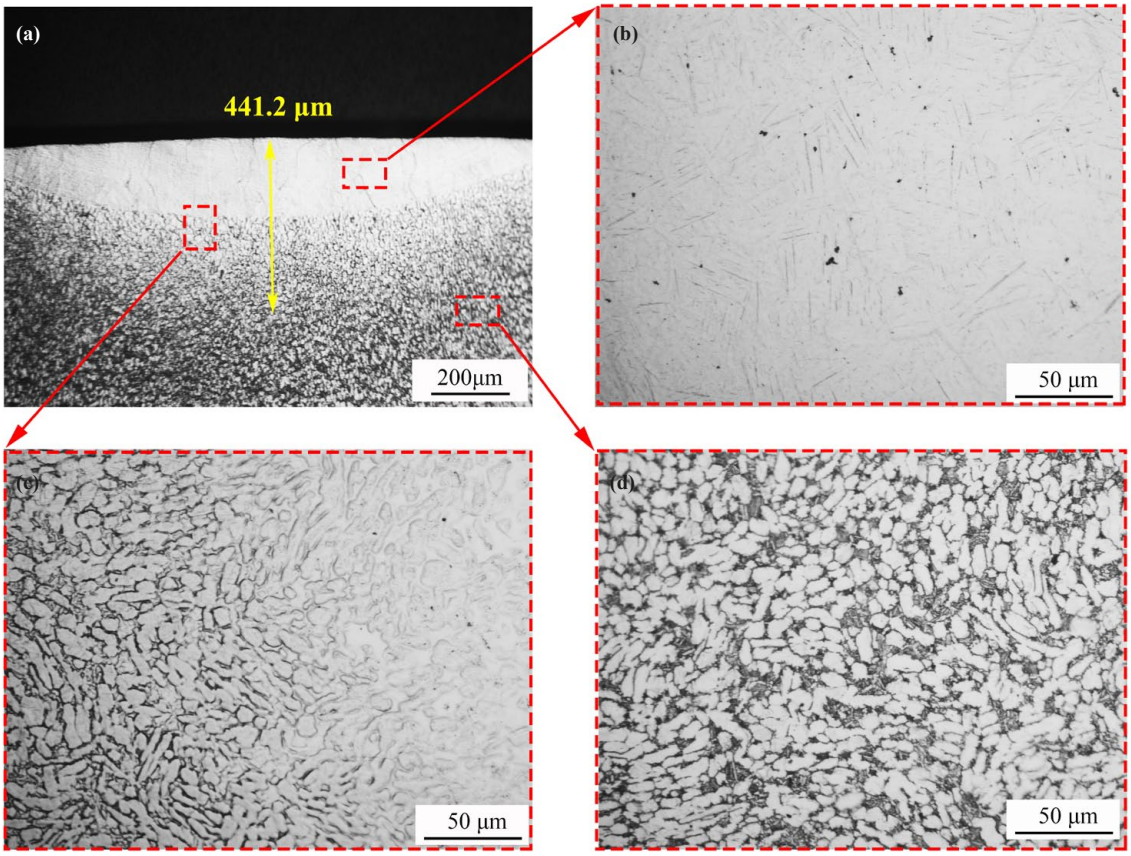

Fig. 6. Cross-section microstructures of the quenched layer (a), microstructures of quenched layer (b), transition region (c), and matrix (d) for TA15 alloy after the laser power treatments of 600 W

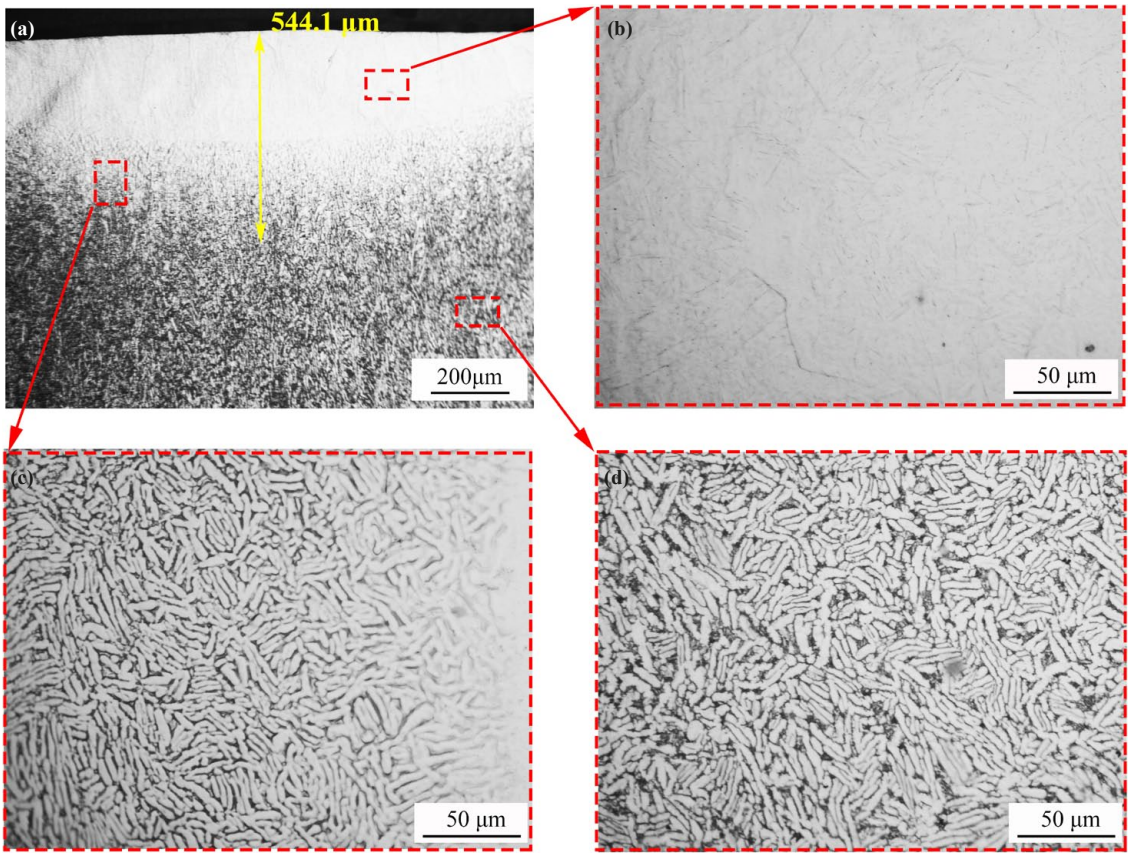

Fig. 7. Cross-section microstructures of the quenched layer (a), microstructures of quenched layer (b), transition region (c), and matrix (d) for TA15 alloy after the laser power treatments of 700 W

alloy at high temperature, which leads to the transformation of β phase into α phase difficultly. Therefore, only the collective regular short-range migration of β phase atoms occurs. The observed results are in complete agreement with those characterized by XRD. This α' martensite belongs to thermally induced martensite rather than stress-induced martensite, which also occurred when Laser quenching was performed on the surface of Ti-35Nb-2Ta-3Zr Alloy [17].

Fig. 5c-8c show the microstructures of transition region for TA15 alloy after different laser power treatment. It can be seen that this regions are composed of transformed β structures and α phases. The black parts are transformed β structures, and the white parts with equiaxed and striped shape are α phases. The closer the quenched layer is, the higher the α phase content is and the less the transformed β structure is. The laser quenching power has no obvious effect on the microstructures of the transition regions. The temperature of the transition regions is higher than the phase transition temperature, so the α + β phases will be transformed into β phase at high temperature under the effect of laser heat. Then, the α phase will precipitate from the β phase during the subsequent rapid cooling process when the laser heat source leaves. At the same time, the α phase would grow and coarsen rapidly due to the high energy of laser treatment.

Fig. 5d-8d are the microstructures of matrix after different laser power treatments, which are composed of transformed β structures and α phases. The content of α phase is 70-80%, mainly in the shape of equiaxed and strip. The transformed β structure is distributed in the grain boundary of α phase. It is obvious that the microstructures of matrix are basically the same as that of the initial tested TA15 alloy after laser treatment, and it is not affected by the laser heat.

Fig. 9 shows the SEM images and corresponding element distribution of the surface for TA15 alloy after 800 W laser quenching. There are obvious three regions with different microstructures including the matrix of the inner layer (region C), the transition region in the middle (region D) and the quenched layer of the outer layer (region E). This is similar to the morphologies observed in Fig. 8. In the matrix alloy, typical α and transformed β structures can be observed, with small needle-like secondary α phases forming in the transformed β structures regions. The microstructures of the quenched layer in region E indicate that an obvious martensite structure has been formed on the surface after laser treatment. The element distribution results of map scanning (Fig. 9b-9e) show that the elements of the matrix, the transition region, and the quenched layer are evenly distributed and they are all composed of Ti, Al, Mo, Zr, and V elements. Especially in Fig. 9b, the dashed line is the dividing line between the martensitic structure and α + transformed β structures. It can be seen that there is no obvious difference in the element distribution between these two structures. This indicates that laser quenching treatment does not change the element distribution of TA15 alloy significantly, but only partial element diffusion occurs, resulting in the slight fluctuation of element distribution in the scanning test. The results of elemental

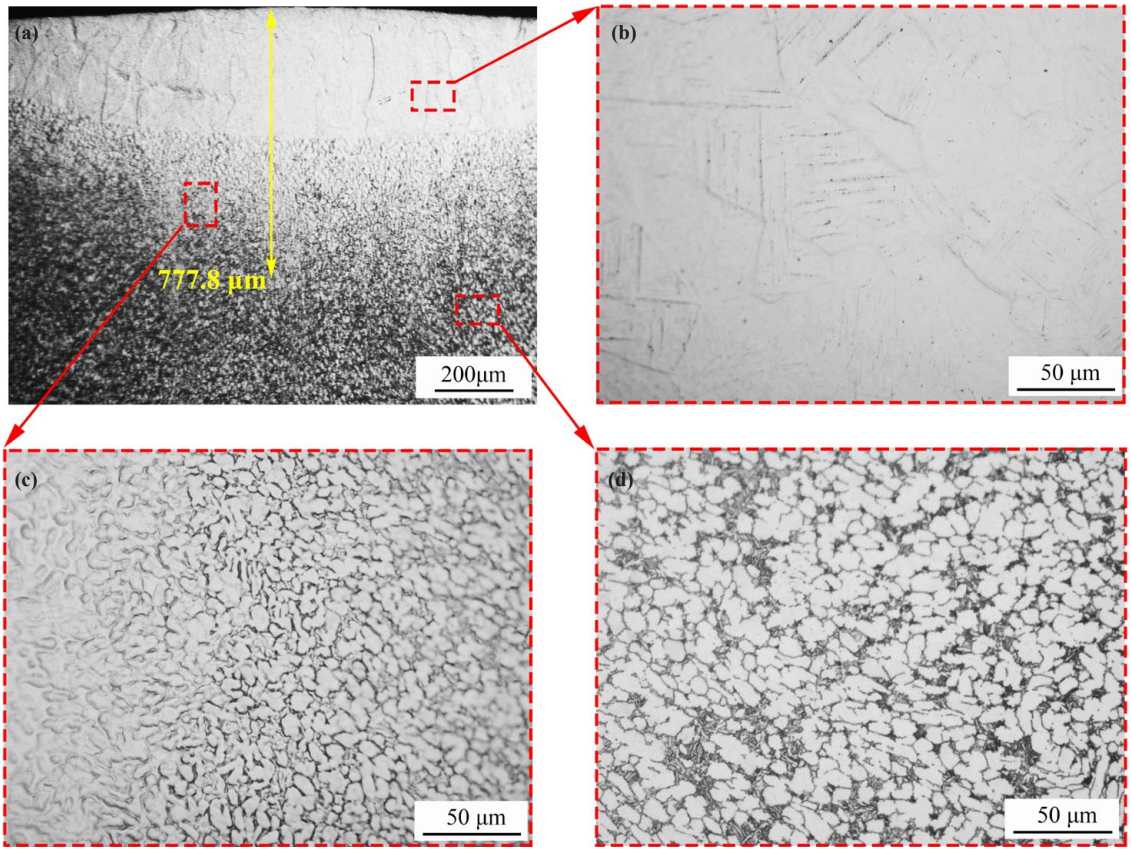

Fig. 8. Cross-section microstructures of the quenched layer (a), microstructures of quenched layer (b), transition region (c), and matrix (d) for TA15 alloy after the laser power treatments of 800 W

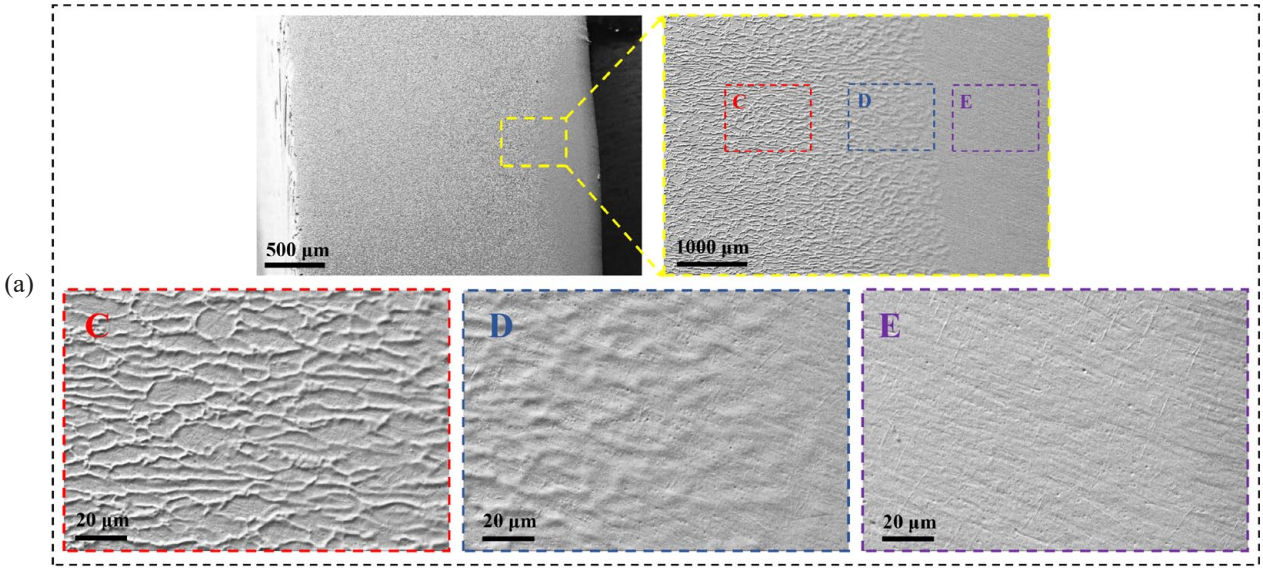
(a)
500 μm
C
D
E
1000 μm
C
20 μm
D
20 μm
E
20 μm

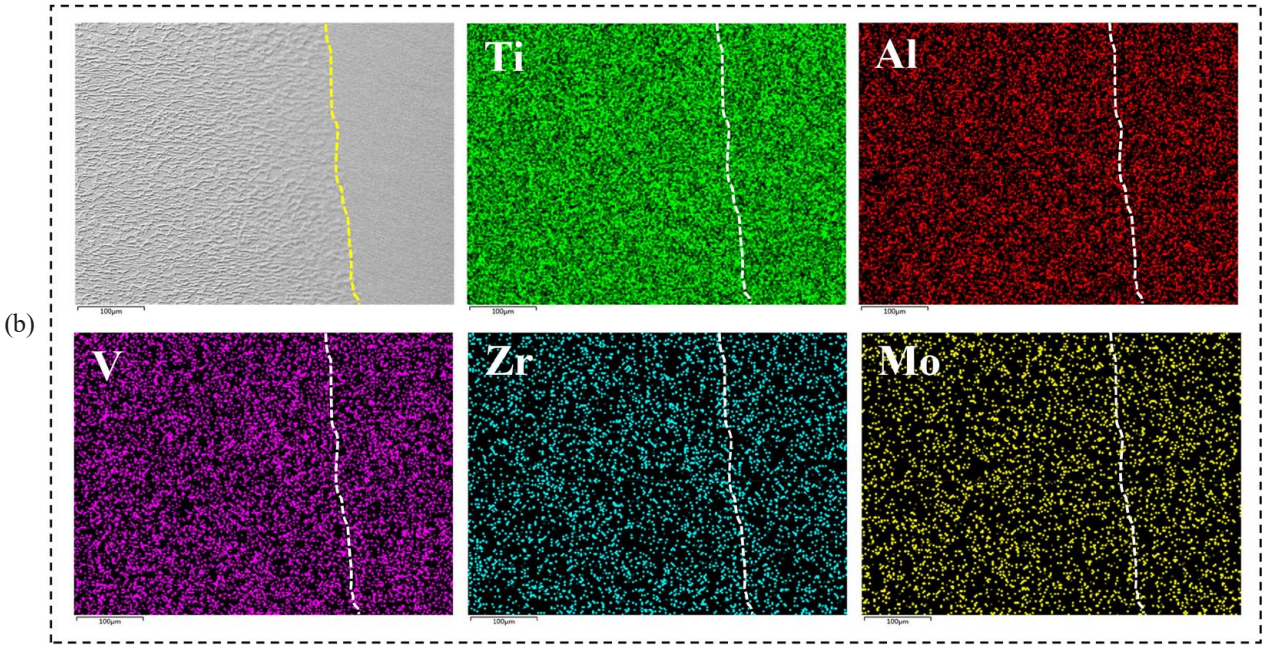
(b)
Ti
Al
V
Zr
Mo

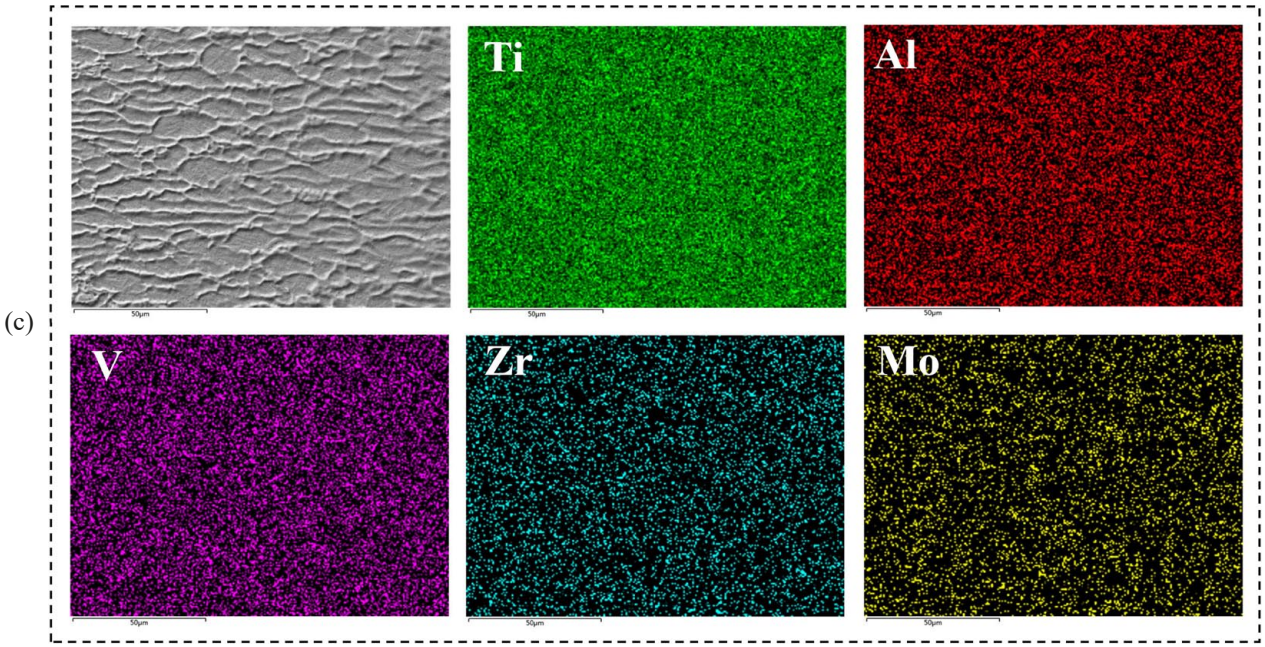
(c)
Ti
Al
V
Zr
Mo

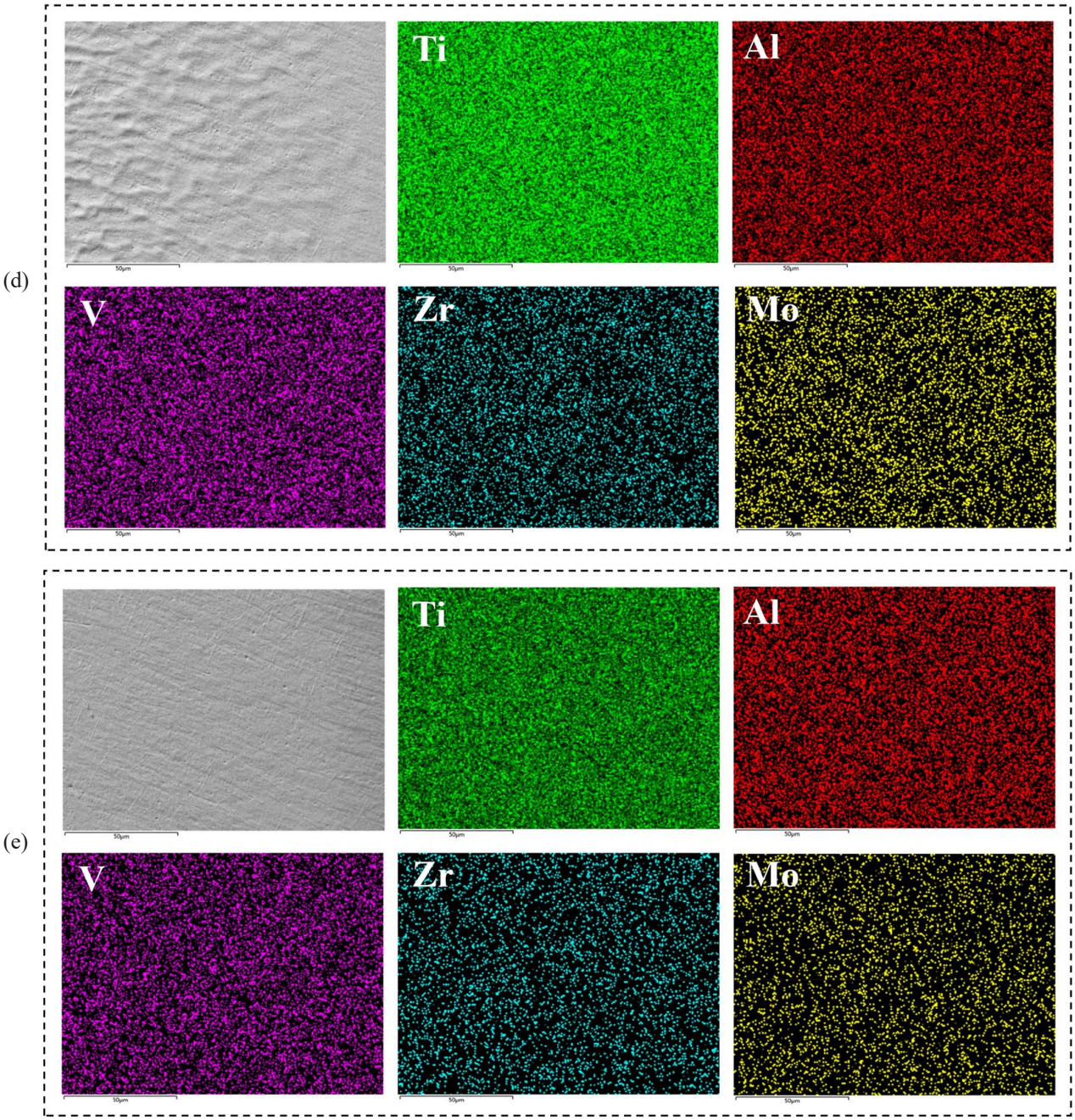

Fig. 9. SEM images and corresponding element distribution of surface for TA15 alloy after 800 W laser quenching. (a) Cross-section microstructures of the quenched layer, microstructures of quenched layer E, transition region D, and matrix C. Element distribution of the surface for TA15 alloy (b), regions C for matrix alloy (c), regions D for transition region (d) and regions E for the quenched layer (e)

distribution of the matrix (Fig. 9c), the transition region (Fig. 9d), and the quenched layer (Fig. 9e) also confirmed this conclusion. This element undulation of the quenched area indicates dynamics and possible instability of the laser quenching process, and it is the main reason for the microstructures difference.

3.3. Effect of laser quenching on hardening layer

Fig. 5a-8a are the cross-section microstructures of TA15 alloy after different laser power treatment. Because the hardening phases α and α' are also formed in the transition region, the thickness of the quenched layer and half of the transition region is taken as the thickness of the hardening layer in this work. As shown in Fig. 5a-8a, the measured thicknesses of the hardening layer under the laser quenching power of 500 W, 600 W, 700 W and 800 W are 397 μm, 441 μm, 544.1 μm and 777 μm, respectively. The thickness and width of the hardening layer of TA15 alloy after laser quenching treatment are listed in TABLE 3. The results indicate that the thickness and width of hardening layer increases with the increase of laser quenching power. The thicker the hardening layer, the wider its width.

Fig. 10 shows the microhardness curves of quenched surface of TA15 alloy after laser quenching treatment with different pow-

TABLE 3

Thickness and width of the hardening layer of TA15 alloy after laser quenching treatment

Laser power (W)	Thickness (μm)	Width (μm)	
		Microstructures measurement method	Hardness measurement method
500	397	1264±15	1500±18
600	441	1588±24	1700±22
700	544	2000±20	2000±15
800	777	2117±16	2300±20

ers. It is worth noting that the hardness tests were performed on the surface of the samples (shown in Fig. 4b). It can be found that the average hardness of the matrix which is 3 ~ 4 mm away from the quenching center (at point '0' in Fig. 10) is between 320 $HV_{0.3}$ and 370 $HV_{0.3}$, while the average hardness of the martensite hardening layer (0.5 mm away from the quenching center) can reach more than 430 $HV_{0.3}$. The average hardness of the transition region (heat affected zone) is about 400 $HV_{0.3}$. When the Vickers hardness value is 300 $HV_{0.3}$-450 $HV_{0.3}$, the average indentation size is about 30-45 μm, which is smaller than the spacing between the indentations (500 μm) in this hardness test. This shows that the measurement of hardness value is not affected by the indentation spacing in this work. The width of the hardening layer can be measured according to the hardness results, and the results are shown in TABLE 3. It is clear that the widths of the hardening layer obtained by the methods of microstructures and hardness measurements are basically the same, which suggests that the results of this work are reliable. Compared with the matrix alloy, the surface hardness of the TA15 alloy after laser quenching is increased by nearly 40%. The increase of surface hardness will play an active role in the wear resistance of the TA15 alloy. This increase in hardness was also found in Ti-6.5Al-1.5Zr-3.5Mo-0.3Si (TC11) alloy [20] and Ti-35Nb-2Ta-3Zr alloy [17] after laser quenching. This may be due to the fact that both TA15 and TC11 alloy

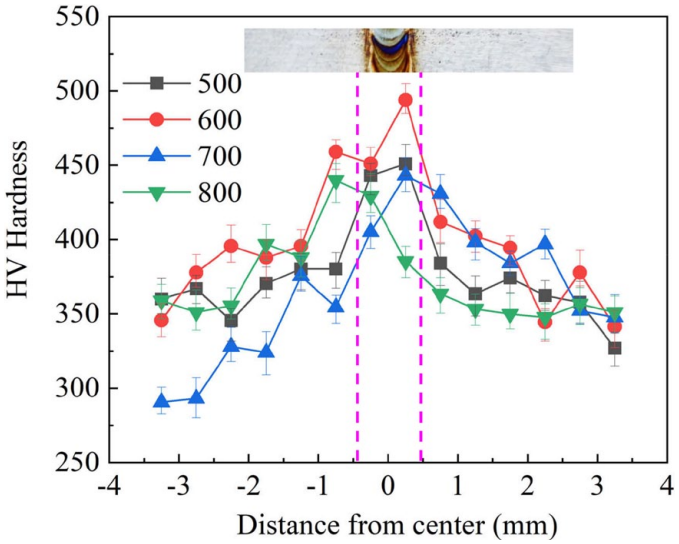

Fig. 10. Microhardness of quenched surface of TA15 alloy treated with different laser powers

form equiaxed α phases and transformed β structures, while there are equiaxed grains forming in the Ti-35Nb-2Ta-3Zr alloy. It can be seen that the increase of surface hardness of titanium alloy after laser quenching depends on the microstructures of the alloy.

It can be seen from Fig. 10 that the hardness shows an increasing trend after laser quenching from the matrix to the transition region and then to the quenched layer. Because the matrix is hardly affected and no phase transition occurs after laser quenching treatment, hence, the hardness of matrix will not change due to the unchanged microstructures. After laser quenching, the hexagonal martensite α'-Ti is formed in the quenched layer through nondiffusion transformation, resulting in obvious solution strengthening effect and increased intrinsic stress due to lattice distortion and grain refinement effect. This α'-Ti significantly increases the hardness of the quenched layer. The α phase formed by the cooling of β phase in the transition region can also improve the hardness. Therefore, the hardness of the surface for TA15 alloy after laser quenching treatment presents a gradient change, and reaches the maximum value in the quenched layer.

4. Conclusions

(1) After laser quenching treatment, TA15 alloy is composed of hexagonal α phase and hexagonal α' phase. The morphologies of TA15 alloy from the surface to the matrix are martensite α'-Ti of the quenched layer, α-Ti and transformed β structure of the transition region, and α-Ti and transformed β structure of the matrix.

(2) With the increase of laser quenching power, the thickness and width of the surface hardening layer of TA15 alloy increase. The thickness of hardening layer can reach 777 μm when the power is 800W. The hardness of TA15 alloy reaches the maximum value in the quenched layer due to the formation of martensite α'-Ti.

Acknowledgments

This research was supported by the Liaoning Revitalization Talents Program (No. XLYC2007075), and Liaoning Provincial Natural Science Foundation of China (No. 2023-MS-240).

REFERENCES

[1] K. Hua, H. Ding, L. Sun, Y. Cao, X. Li, H. Wu, H. Wang, Enhancing high-temperature fretting wear resistance of TC21 titanium alloys by laser cladding self-lubricating composite coatings. J. Alloy Compd. **977**, 173360 (2024). DOI: https://doi.org/10.1016/j.jallcom.2023.173360

[2] M. Zhang, B. Tang, W. Chen, K. Li, Y. Xie, B. Yin, J. Li, Slip analysis and mechanical deformation behavior in dual-phase tita-

nium alloy: Integrating crystal plasticity simulations with in-situ micro-compression. Mat. Sci. Eng. A, **892**, 146061 (2024). DOI: https://doi.org/10.1016/j.msea.2023.146061

[3] H. Xiao, X.G. Fan, M. Zhan, B.C. Liu, Z.Q. Zhang, Flow stress correction for hot compression of titanium alloys considering temperature gradient induced heterogeneous deformation. J. Mater. Process. Technol. **288**, 116868 (2021). DOI: https://doi.org/10.1016/j.jmatprotec.2020.116868

[4] R. Ji, K. Zhu, H. Zhang, H. Luo, J. Mao, Microstructure evolution, mechanical response and strengthening models for TA15 titanium alloy during thermal processes: A brief review. J. Mater. Res. Technol. **28**, 1644-1656 (2024). DOI: https://doi.org/10.1016/j.jmrt.2023.12.099

[5] Y. Zhang, Z. Zhai, Z. Wu, W. Lin, R. Yang, Z. Zhang, Tailoring high-temperature mechanical properties of laser powder bed fusion Ti-6.5Al-2Zr-1Mo-1 V alloy via microstructure design. Mater. Design **236**, 112488 (2023). DOI: https://doi.org/10.1016/j.matdes.2023.112488

[6] K. Wang, M. Kopec, S. Chang, B. Qu, J. Liu, D.J. Politis, L. Wang, G. Liu, Enhanced formability and forming efficiency for two-phase titanium alloy by Fast light Alloys Stamping Technology (FAST). Mater. Des. **194**, 108948 (2020). DOI: https://doi.org/10.1016/j.matdes.2020.108948

[7] X.Q. Jiang, X.G. Fan, M. Zhan, R. Wang, Y.F. Liang, Microstructure dependent strain localization during primary hot working of TA15 titanium alloy: Behavior and mechanism. Mater. Des. **203**, 109589 (2021). DOI: https://doi.org/10.1016/j.matdes.2021.109589

[8] Y. Li, P. Gao, J. Yu, S. Jin, S. Chen, M. Zhan, Mesoscale deformation mechanisms in relation with slip and grain boundary sliding in TA15 titanium alloy during tensile deformation. J. Mater. Sci. Technol. **98**, 72-86 (2022). DOI: https://doi.org/10.1016/j.jmst.2021.05.008

[9] J. Zhao, L. Lv, G. Liu, K. Wang, Analysis of deformation inhomogeneity and slip mode of TA15 titanium alloy sheets during the hot tensile process based on crystal plasticity model. Mat. Sci. Eng. A **707**, 30-39 (2017). DOI: https://doi.org/10.1016/j.msea.2017.08.094

[10] M.S. Baltatu, C. Chiriac-Moruzzi, P. Vizureanu, L. Tóth, J. Novák, Effect of Heat Treatment on Some Titanium Alloys Used as Biomaterials. Appl. Sci. **12**, 11241 (2022). DOI: https://doi.org/10.3390/app122111241

[11] D.S. Fernández, B.P. Wynne, P. Crawforth, M. Jackson, Titanium alloy microstructure fingerprint plots from in-process machining. Mat. Sci. Eng. A **811**, 141074 (2021). DOI: https://doi.org/10.1016/j.msea.2021.141074

[12] Y. Wang, Z. Sun, Z. Yin, L. Yin, L. Huang, Formation and characteristics of bilamellar microstructure in Ti6242S titanium alloy under dual heat treatment. Mater. Charact. **187**, 111835 (2022). DOI: https://doi.org/10.1016/j.matchar.2022.111835

[13] S. Huang, X. Ming, Y. Hu, Q. Zhang, Y. Tang, S. Zhang, W. Chen, X. Lin, Microstructural evolution during post-heat treatment and its effect on the mechanical properties of directed energy deposited near β titanium alloy. J. Alloy Compd. **934**, 168001 (2023). DOI: https://doi.org/10.1016/j.jallcom.2022.168001

[14] R. Sola, P. Veronesi, R. Giovanardi, G. Parigi, A Novel Duplex Treatment of C20 Steel Combining Low-Pressure Carburizing and Laser Quenching. J. Mater. Eng. Perform. **26**, 5396-5403 (2017). DOI: https://doi.org/10.1007/s11665-017-2965-3

[15] Z.X. Li, B.Q. Tong, Q.L. Zhang, J.H. Yao, V. Kovalenko, Microstructure refinement and properties of 1.0C-1.5Cr steel in a duplex treatment combining double quenching and laser surface quenching. Mat. Sci. Eng. A **776**, 138994 (2020). DOI: https://doi.org/10.1016/j.msea.2020.138994

[16] C. Chen, A. Feng, B. Liu, Y. Wei, X. Song, Effect of quench-tempering and laser quenching on the microstructure and properties of high-chromium cast iron. J. Mater. Res. Technol. **19**, 2759-2773 (2022). DOI: https://doi.org/10.1016/j.jmrt.2022.06.022

[17] T. Zhang, Q. Fan, X. Ma, W. Wang, K. Wang, P. Shen, J. Yang, Microstructure and Mechanical Properties of Ti-35Nb-2Ta-3Zr Alloy by Laser Quenching. Front. Mater. **6**, 318 (2019). DOI: https://doi.org/10.3389/fmats.2019.00318

[18] X. Zong, Z.L. Jing, L.X. Cheng, H. Tang, H. Wang, Non-isothermal β grain growth behaviour of pure titanium under laser quenching. Mater. Sci. Tech-lond. **36**, 668-673 (2020). DOI: https://doi.org/10.1080/02670836.2020.1729498

[19] Q.T. Yao, C. Tian, J. Sun, L. Zuo, W.P. Tong, Microstructure and properties of nitrided layer of titanium plate, produced by simultaneous laser quenching and liquid-nitrogen cryogenics. Sci. China Technol. **61**, 1901-1906 (2018). DOI: https://doi.org/10.1007/s11431-018-9293-9

[20] H. Zhang, X. Yang, H. Cui, W. Wen, Study on the Effect of Laser Quenching on Fretting Fatigue Life. Metals **9** (5), 566 (2019). DOI: https://doi.org/10.3390/met9050566

[21] Shaolong Li, Shufeng Li, Lei Liu, Lina Gao, Yabo Fu, Xin Zhang, Bo Li, High temperature softening mechanism of powder metallurgy TA15 alloy. Materials Science & Engineering A **877**, 145160 (2023). DOI: https://doi.org/10.1016/j.msea.2023.145160

[22] Q.J. Sun, X. Xie, Microstructure and mechanical properties of TA15 alloy after thermomechanical processing. Materials Science & Engineering A **724**, 493-501 (2018). DOI: https://doi.org/10.1016/j.msea.2018.03.109